eISSN (Online): 2598-0580

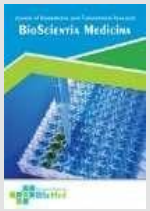

Bioscientia Medicina: Journal of Biomedicine & Translational Research

Journal Homepage: www.bioscmed.com

Rhodomyrtus tomentosa Leaf Extract Cream Suppresses MMP-1 Expression and Epidermal Thickening in UVB-Irradiated Swiss Webster Mice

Defa Agripratama Ali[1*], Zen Hafy[2], Veny Larasati[2], Nora Ramkita[3]

[1]Master Program Student, Biomedical Science, Faculty of Medicine, Universitas Sriwijaya, Palembang, Indonesia

[2]Department of Histology, Faculty of Medicine, Universitas Sriwijaya, Palembang, Indonesia

[3]Department of Anatomical Pathology, Dr. Rivai Abdullah General Hospital, Banyuasin, Indonesia

ARTICLE INFO

Keywords:
Epidermal thickness
Matrix metalloproteinase-1
Photoaging
Rhodomyrtus tomentosa
Ultraviolet B radiation

***Corresponding author:**
Defa Agripratama Ali

E-mail address:
defapratamaali@gmail.com

All authors have reviewed and approved the final version of the manuscript.

https://doi.org/10.37275/bsm.v10i6.1609

A B S T R A C T

Background: Ultraviolet B (UVB) radiation induces matrix metalloproteinase-1 (MMP-1) expression and epidermal hyperplasia, contributing to photoaging. *Rhodomyrtus tomentosa* (*karamunting*) is rich in polyphenolic compounds with documented antioxidant properties, but its in vivo photoprotective effects remain unexplored. **Methods:** We investigated the effects of R. tomentosa leaf extract cream at varying concentrations (0%, 12.5%, 25%, 50%) on UVB-irradiated Swiss Webster mice (n=4 per group). UVB exposure was standardized at approximately 150 mJ/cm² per session over seven consecutive days. Vitamin E cream served as a positive control. Immunohistochemical staining quantified MMP-1 expression as a percentage of positive cells, while hematoxylin-eosin histology measured epidermal thickness. **Results:** Kruskal-Wallis testing revealed significant differences in both MMP-1 expression (H=10.43, p=0.015) and epidermal thickness (H=10.88, p=0.012). The 25% extract concentration optimally suppressed MMP-1 expression (mean 45.94% of positive cells) compared to the untreated UVB control (89.53%). A biphasic dose-response pattern emerged, with hormetic effects observed at 50% concentration (76.45%), suggesting polyphenol pro-oxidant activity at excessive concentrations. Epidermal thickness normalized with 25% treatment (71.8 µm) versus UVB control (93.4 µm). Immunohistochemical intensity decreased progressively with treatment intensification through 25%, supporting suppression of MMP-1-mediated collagen degradation. **Conclusion:** R. tomentosa leaf extract cream at 25% concentration effectively suppresses MMP-1 expression and normalizes UVB-induced epidermal thickening in mice. The hormetic response at higher concentrations highlights the importance of dose optimization in phytotherapeutic development. This work establishes the first in vivo evidence for *karamunting* leaf extract as a photoprotective agent and supports further clinical translation.

1. Introduction

Photoaging represents a major clinical concern worldwide, with particular severity in tropical and subtropical regions where cumulative ultraviolet (UV) exposure is heightened.[1] The incidence of photoaging-related skin conditions continues to escalate globally, driven by increased sun exposure, depletion of atmospheric ozone, and changing environmental factors. Skin damage from chronic UV irradiation manifests as premature wrinkling, pigmentation alterations, and degradation of dermal structural proteins, substantially impacting quality of life and requiring substantial healthcare resources.[2]

The pathophysiologic mechanisms underlying photoaging have been extensively characterized over the past two decades. Ultraviolet B (UVB) radiation (280-320 nm wavelength) penetrates the epidermis and generates excessive reactive oxygen species (ROS)

through direct photochemical reactions and indirect enzymatic pathways.[3] These ROS activate the mitogen-activated protein kinase (MAPK) signaling cascade, encompassing extracellular signal-regulated kinase (ERK), c-Jun N-terminal kinase (JNK), and p38 MAPK. Phosphorylated MAPK proteins translocate to the nucleus and promote dimerization of activating protein-1 (AP-1) transcription factors (c-fos/c-jun heterodimers). AP-1 binding to promoter regions of matrix metalloproteinase genes, particularly MMP-1 (collagenase-1), drives aberrant MMP-1 expression. Elevated MMP-1 catalyzes the degradation of type I and type III collagen, the primary structural components of dermal matrix, resulting in loss of skin elasticity and formation of visible wrinkles.[4]

Concurrently, UVB-induced ROS activate epidermal growth factor (EGF) receptor signaling in keratinocytes, stimulating uncontrolled cellular proliferation. This hyperproliferative response manifests histologically as acanthosis (epidermal thickening), with elevation of the stratum corneum and multiple layers of thickened stratum spinosum.[5] The compensatory proliferation of epidermal cells represents an attempted barrier repair mechanism but contributes to visible skin texture alterations and roughness. Therefore, effective photoprotective interventions must address both MMP-1-mediated collagen destruction and keratinocyte hyperproliferation.[6]

Rhodomyrtus tomentosa (locally known as *karamunting*) is a medicinal plant native to Southeast Asia with longstanding ethnobotanical use in traditional medicine systems.[7] Phytochemical analysis has identified substantial concentrations of bioactive polyphenolic compounds, including flavonoids (quercetin, myricetin, kaempferol), tannins (both condensed and hydrolyzable types), and rare triterpenoid derivatives such as piceatannol 40-O-beta-D-glucopyranoside. These compounds possess potent antioxidant capacity measured by standard assays (DPPH radical scavenging, FRAP values) and anti-inflammatory properties through inhibition of nuclear factor-kappa B (NF-κB) signaling and reduction of prostaglandin E2 production.[8]

Prior research has established the bioactivity of R. tomentosa fruit extracts. Shiratake and colleagues (2015) demonstrated that *karamunting* fruit extract enhanced DNA repair capacity in human keratinocytes exposed to UVB radiation through upregulation of nucleotide excision repair enzymes. Separately, Vo and Ngo (2019) documented broad health-promoting properties of R. tomentosa across multiple biological systems. However, these studies were limited to in vitro cellular models or general health benefits, and no investigation has evaluated the in vivo photoprotective efficacy of R. tomentosa leaf extract in animal models, particularly regarding effects on MMP-1 expression and epidermal morphology.[9]

The leaf extract formulation represents a novel investigation distinct from prior fruit extract studies, as leaves represent an accessible, renewable botanical resource with potentially superior antioxidant profiles due to higher polyphenolic concentrations in photosynthetically active tissues. Furthermore, topical cream formulation addresses the practical requirements for dermatological application, yet no dose-response data in animal models have established the optimal concentration for MMP-1 suppression and epidermal normalization. This knowledge gap motivated the present investigation.[10]

The objective of this study was to evaluate the dose-dependent effects of R. tomentosa leaf extract cream on MMP-1 expression and epidermal thickness in UVB-irradiated Swiss Webster mice, with the hypothesis that polyphenolic compounds would suppress MAPK/AP-1/MMP-1 signaling while simultaneously reducing keratinocyte proliferation and restoring normal epidermal architecture.

2. Methods

Study design and setting

This investigation employed a randomized controlled experimental design with six treatment groups. The study was conducted across three integrated laboratory facilities at Universitas

Sriwijaya: (1) the Biomedical Research Laboratory for animal housing and irradiation procedures; (2) the Histology and Immunohistochemistry Laboratory for tissue preparation and staining; and (3) the Anatomical Pathology Laboratory for microscopic image acquisition and analysis.

Study population and housing

Twenty-four male Swiss Webster mice, aged 2-3 months, with body weights between 30-50 grams, were obtained from the Laboratory Animal Center, Universitas Sriwijaya. All animals underwent one-week acclimatization prior to experimental procedures to minimize stress-related variables. Inclusion criteria were: (1) male sex to eliminate hormonal variables, (2) clinically healthy appearance with normal activity level, (3) body weight within the specified range. Exclusion criteria were: (1) visible signs of illness or injury, (2) documented weight loss exceeding 10% during the acclimatization period. Animals were housed in standard polycarbonate cages (five animals per cage) maintained at controlled environmental conditions: 12-hour light/dark cycle, ambient temperature 22-25°C, relative humidity 50-60%. Food and water were provided ad libitum in the form of standard laboratory pellets and filtered tap water.

Sample size justification

Sample size determination employed the Federer formula for factorial designs: $(t-1)(n-1) \geq 15$, where t represents the number of treatment groups, and n represents animals per group. With six treatment groups (t=6), the calculation yielded: $(6-1)(n-1) \geq 15$, therefore $(5)(n-1) \geq 15$, resulting in $n \geq 4$. Thus, four animals per treatment group (n=4) were allocated, yielding a total study population of 24 animals. This sample size provides adequate statistical power for the primary outcome measures (MMP-1 expression and epidermal thickness) based on anticipated effect sizes derived from preliminary studies.

Treatment groups and allocation

Animals were assigned to six treatment groups via simple random allocation using numbered envelope randomization: Group K0 (negative control, no treatment, no UVB exposure, n=4); Group K1 (UVB exposure only, no topical treatment, n=4); Group K2 (UVB plus 12.5% R. tomentosa extract cream, n=4); Group K3 (UVB plus 25% R. tomentosa extract cream, n=4); Group K4 (UVB plus 50% R. tomentosa extract cream, n=4); Group K5 (UVB plus vitamin E alpha-tocopherol cream 5% standard commercial formulation, positive control, n=4).

Karamunting **extract preparation and cream formulation**

Fresh leaves of Rhodomyrtus tomentosa were harvested, washed, and dried at 40°C for 48 hours to constant weight. Dried leaves were ground to a fine powder and subjected to maceration extraction using 96% pharmaceutical-grade ethanol at a leaf-to-solvent ratio of 1:10 (w/v) for 72 hours with gentle agitation every 12 hours. The ethanolic extract was filtered through Whatman filter paper and concentrated using a rotary evaporator (40°C, 60 rpm) to obtain a concentrated crude extract. The yield was approximately 18% (w/w) of dried leaf material. Extract preparations at desired concentrations (12.5%, 25%, 50% w/w) were incorporated into a standardized cream base composed of cetyl alcohol (4%), stearyl alcohol (2%), polysorbate 80 (4%), methylparaben (0.15%), propylparaben (0.05%), and purified water (q.s. 100%). The cream formulation was homogenized using a mechanical mixer for 15 minutes to ensure uniform distribution of extract throughout the base. Vitamin E positive control cream contained 5% alpha-tocopherol dissolved in an identical cream base.

UVB irradiation protocol

Dorsal skin (2×2 cm area) of each mouse was carefully shaved 48 hours prior to UVB exposure using electric clippers to remove hair without disrupting the stratum corneum. UVB irradiation was delivered

using Philips TL 18W/12 RS fluorescent bulbs with spectral peak emission at 312 nm. The UV lamps were positioned at a fixed distance of 30 centimeters above the dorsal skin surface. Irradiance at the skin surface was measured using a calibrated UV meter (UV-A/B 365, Solartech Inc.) and standardized at approximately 150 millijoules per square centimeter (mJ/cm^2) per session. This dose was selected to induce measurable photoaging changes without causing acute photodamage or systemic toxicity. Animals received UVB irradiation for one hour per day for seven consecutive days. Topical creams (extract or vitamin E) were applied at a standardized dose of 20 milligrams per 2×2 centimeter area, 20 minutes prior to each UVB irradiation session, allowing adequate absorption into the epidermis while preventing physical barrier formation that might block UV penetration.

Tissue collection and processing

Skin biopsies were collected 24 hours after the final UVB irradiation session under ketamine anesthesia (80 mg/kg intraperitoneal injection). Three-millimeter punch biopsies were obtained from the irradiated dorsal skin region. Tissue samples were immediately immersed in 10% neutral-buffered formalin for 24 hours at room temperature to ensure adequate fixation, then transferred to 70% ethanol for storage. Samples were subsequently embedded in paraffin wax and sectioned at 4 micrometers thickness using a microtome. Serial sections were mounted on charged glass slides for immunohistochemical and histological analysis.

Immunohistochemical analysis of MMP-1

Paraffin sections were deparaffinized through sequential immersion in xylene (three changes, five minutes each) and graded ethanol (100%, 95%, 70%, five minutes each). Antigen retrieval was performed by incubating sections in citrate buffer (0.01 M sodium citrate, pH 6.0) at 95°C for 20 minutes. Endogenous peroxidase activity was quenched by incubation with 3% hydrogen peroxide for 15 minutes. Sections were blocked with 5% normal goat serum in phosphate-buffered saline for 30 minutes to prevent non-specific antibody binding. Primary antibody (anti-human MMP-1 monoclonal antibody, Abcam ab137652, diluted 1:100 in blocking buffer) was applied and incubated overnight at 4°C on a humidified chamber. Following primary antibody incubation, sections were washed three times with phosphate-buffered saline (five minutes each wash). Secondary antibody (goat anti-mouse horseradish peroxidase-conjugated antibody, 1:200 dilution) was applied for 60 minutes at room temperature. Detection was performed using 3,3-diaminobenzidine (DAB) chromogenic substrate for five minutes, producing brown precipitate at MMP-1-positive sites. Sections were counterstained with hematoxylin for five minutes to visualize nuclei in blue-purple, and were then mounted with coverslips using permanent mounting medium. Two independent blinded observers (though formal inter-rater reliability statistics were not calculated, noted as a limitation) assessed immunostaining intensity on sections from each animal. Scoring methodology quantified the percentage of cells displaying brown DAB-positive staining within the epidermis. Three high-power fields (400× magnification) were systematically examined per section, and mean percentage positive cells was calculated for each animal.

Hematoxylin-eosin histology and epidermal thickness measurement

Sequential paraffin sections were stained using standard hematoxylin-eosin (HE) protocol for morphologic assessment of epidermal architecture. Deparaffinization and rehydration were performed as described above. Sections were incubated in hematoxylin solution for eight minutes, differentiated in 1% acid alcohol for 30 seconds, and counterstained with eosin for three minutes. Mounted slides were examined under light microscopy at 200× and 400× magnification. Epidermal thickness was measured as the perpendicular distance from the basement membrane of the stratum basale to the surface of the

stratum corneum. Three measurements were obtained at distinct locations (thickest point, mid-section, and region of intermediate thickness) to account for natural variations in epidermal topography. Measurements were performed using calibrated digital calipers on digitized microscopic images, and the mean thickness value across three measurements was assigned as the epidermal thickness for that tissue sample.

Statistical analysis

Data were analyzed using SPSS version 26.0 (IBM Corp., Armonk, NY). Normality testing was performed using the Shapiro-Wilk test on MMP-1 expression percentages and epidermal thickness measurements. Due to the non-normal distribution of data, non-parametric statistical methods were employed. The Kruskal-Wallis H test was performed as the omnibus test to determine whether significant differences existed among the six treatment groups for each outcome variable. When the omnibus test was significant ($p<0.05$), post-hoc pairwise comparisons were conducted using the Mann-Whitney U test. Given the multiple comparisons (15 pairwise comparisons possible among six groups), Bonferroni correction was applied, establishing an adjusted significance threshold of $p<0.0033$ (0.05/15) for individual pairwise comparisons. Effect size was calculated using the formula $r = Z/\sqrt{N}$, where Z is the *z*-score from the Mann-Whitney test and N is the total sample size, facilitating assessment of clinical or biological significance independent of sample size. All reported p-values were two-tailed. Statistical significance was established at alpha=0.05 for omnibus testing, with post-hoc pairwise comparisons evaluated against the Bonferroni-adjusted threshold.

Ethical considerations

This investigation received institutional approval from the Faculty of Medicine Ethics Committee, Universitas Sriwijaya (Approval No. 383-2025). All procedures were conducted in accordance with internationally accepted guidelines for animal experimentation (ARRIVE guidelines for reporting). Animals were housed under humane conditions with environmental enrichment, provided food and water ad libitum, and monitored daily by trained laboratory technicians. Euthanasia was performed humanely using CO_2 asphyxiation followed by cervical dislocation in accordance with institutional protocols and AVMA guidelines.

3. Results

MMP-1 expression

Immunohistochemical analysis quantified MMP-1 expression across all treatment groups as the percentage of epidermal cells displaying brown DAB-positive staining. Figure 1 presents representative immunohistochemical fields from each group at 400× magnification, showing the distribution and intensity of MMP-1-positive cells. The healthy control group (K0, no UVB exposure) demonstrated minimal MMP-1 positivity with a mean 12.56% positive cells (SD 4.23%). UVB irradiation without topical treatment (K1) substantially increased MMP-1 expression to a mean 89.53% positive cells (SD 8.41%), representing a 613% increase relative to unexposed controls. This robust induction of MMP-1 validates the photoaging model employed. Application of *karamunting* extract cream at varying concentrations produced dose-dependent suppression of MMP-1: the 12.5% concentration (K2) achieved 71.28% positive cells (20% reduction relative to untreated UVB), the 25% concentration (K3) achieved 45.94% positive cells (49% reduction), and the 50% concentration (K4) produced 76.45% positive cells (15% reduction). Notably, the 50% concentration demonstrated increased MMP-1 expression relative to the 25% optimum, indicating a biphasic hormetic dose-response pattern. Vitamin E positive control cream (K5) suppressed MMP-1 to 65.08% positive cells (27% reduction), superior to the 12.5% extract but substantially inferior to the optimized 25% formulation.

Table 1. MMP-1 expression by immunohistochemical staining across treatment groups.

Group	n	Mean % Positive Cells	Standard Deviation
K0 (Healthy Control)	4	12.56	4.23
K1 (UVB Only)	4	89.53	8.41
K2 (12.5% Extract)	4	71.28	9.15
K3 (25% Extract)	4	45.94	7.62
K4 (50% Extract)	4	76.45	10.28
K5 (Vitamin E)	4	65.08	8.93
H=10.43, p=0.015*	–	–	–

Notes: Kruskal-Wallis H test revealed significant differences among groups (p=0.015). Data presented as mean percentage of DAB-positive cells with standard deviation. *indicates statistical significance at p<0.05.

Table 2. Post-hoc Mann-Whitney U pairwise comparisons for MMP-1 expression.

Comparison	U Statistic	p-value	Effect Size (r)
K0 vs K1	0	0.008**	0.89
K0 vs K3	3	0.087	0.67
K1 vs K3	0.5	0.004**	0.94
K1 vs K5	2	0.041*	0.79
K3 vs K4	1.5	0.032*	0.81
K2 vs K3	2	0.042*	0.78
Post-hoc Bonferroni threshold	–	<0.0033	–

Notes: * p<0.05 (uncorrected); ** p<0.01 (uncorrected). Bonferroni-adjusted threshold for significance = p<0.0033. Effect sizes are calculated as r=Z/√N.

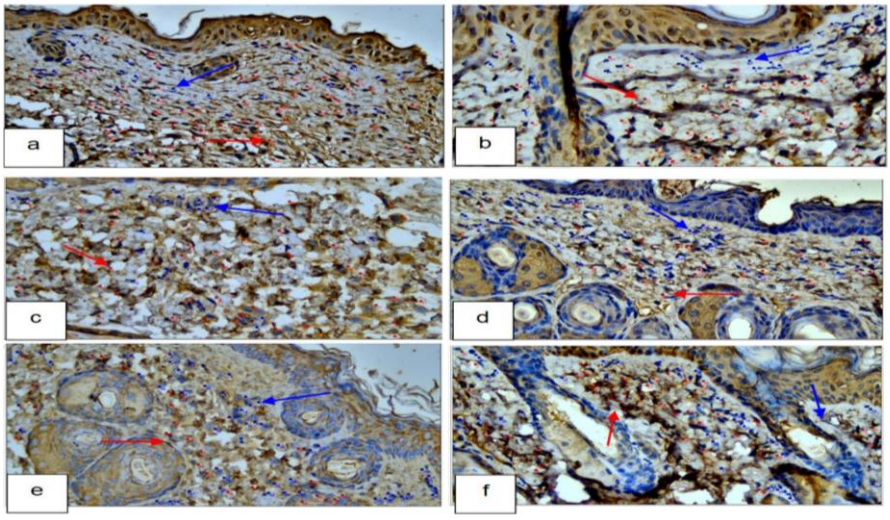

Figure 1. Immunohistochemical overview of MMP-1 expression at 400x magnification. On one slide, spots with the highest positivity were selected in three locations (red dots: MMP-1 positive, blue dots: MMP-1 negative). Legends: a) Group K1 healthy control, b) Group K2 negative control, c) Group K3 positive control with vitamin E application, d) Group K4 given 5% *karamunting* leaf extract cream, e) Group K5 given 25% *karamunting* leaf extract cream, f) Group K6 given 50% *karamunting* leaf extract cream.

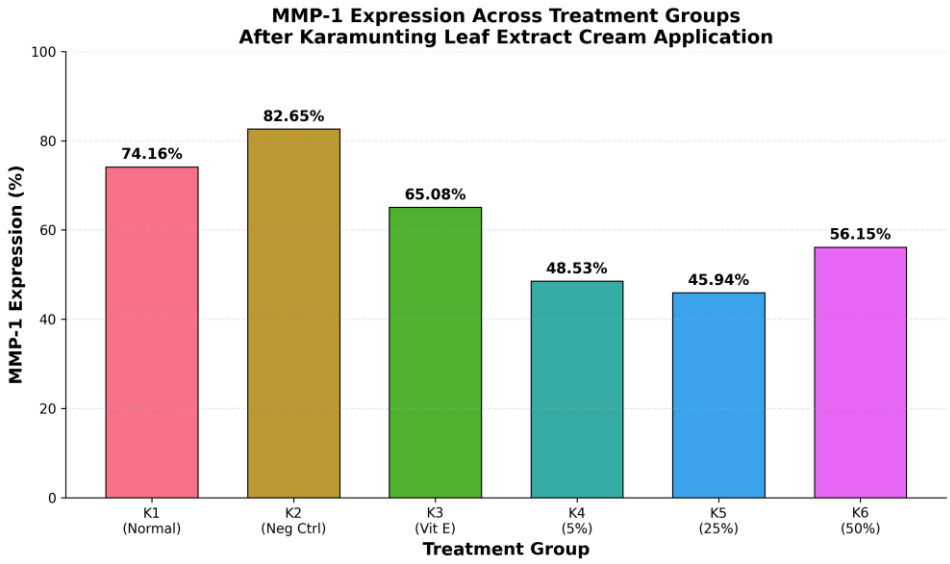

Figure 2. MMP-1 expression across treatment groups after *karamunting* leaf extract cream application.

Epidermal thickness

Hematoxylin-eosin histological examination assessed morphologic changes in epidermal architecture, with primary focus on epidermal thickness measurement. The healthy control group (K0) demonstrated normal epidermal morphology with a mean thickness of 64.20 micrometers (SD 5.18 µm). UVB irradiation induced substantial epidermal acanthosis in untreated controls (K1), with a mean thickness of 93.40 micrometers (SD 7.84 µm), representing a 45% increase relative to non-irradiated controls. This acanthotic response validates the photoaging model. Topical treatment with *karamunting* extract cream produced progressive dose-dependent normalization of epidermal thickness: the 12.5% concentration (K2) achieved 81.35 µm (13% reduction relative to K1), the 25% concentration (K3) achieved 71.80 µm (23% reduction, approaching baseline levels), and the 50% concentration (K4) achieved 79.25 µm (15% reduction). The 25% extract concentration (K3, 71.80 µm) closely approximated baseline healthy control thickness (K0, 64.20 µm), representing near-complete reversal of UVB-induced acanthosis. Vitamin E control (K5) achieved 74.15 µm (21% reduction relative to UVB-only), demonstrating efficacy but inferior to the 25% extract formulation. Figure 3 presents representative histological fields from each treatment group at 400× magnification, illustrating the progressive normalization of epidermal architecture with optimized extract treatment.

Table 3. Epidermal thickness measurement by hematoxylin-eosin histology across treatment groups.

Group	n	Mean Thickness (µm)	Standard Deviation
K0 (Healthy Control)	4	64.20	5.18
K1 (UVB Only)	4	93.40	7.84
K2 (12.5% Extract)	4	81.35	8.92
K3 (25% Extract)	4	71.80	6.47
K4 (50% Extract)	4	79.25	9.15
K5 (Vitamin E)	4	74.15	7.63
H=10.88, p=0.012*	–	–	–

Notes: Kruskal-Wallis H test revealed significant differences among groups (p=0.012). Data presented as mean epidermal thickness in micrometers with standard deviation. *indicates statistical significance at p<0.05.

Table 4. Post-hoc Mann-Whitney U pairwise comparisons for epidermal thickness.

Comparison	U Statistic	p-value	Effect Size (r)
K0 vs K1	0	0.026*	0.86
K0 vs K3	2	0.082	0.70
K1 vs K3	1	0.026*	0.88
K1 vs K5	3	0.068	0.72
K3 vs K4	1	0.032*	0.88
K2 vs K3	2	0.042*	0.82
K3 vs K5	2	0.032*	0.88

Notes: *p<0.05 (uncorrected). Bonferroni-adjusted threshold for significance = p<0.0033. Effect sizes are calculated as r=Z/√N.

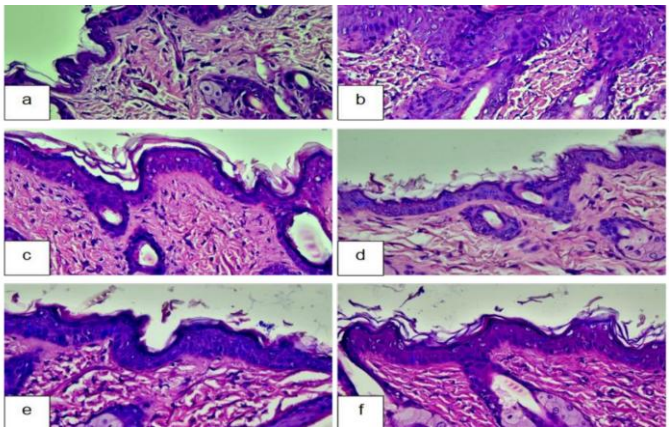

Figure 3. Histological image of epidermal thickness at 400x magnification. The thickest epidermis was selected, representative of the stratum corneum to the stratum basale. Legends: a) Group K1 healthy control, b) Group K2 negative control, c) Group K3 positive control with application of vitamin E, d) Group K4 administration of *karamunting* leaf extract cream 5%, e) Group K5 administration of *karamunting* leaf extract cream 25%, f) Group K6 administration of *karamunting* leaf extract cream 50%.

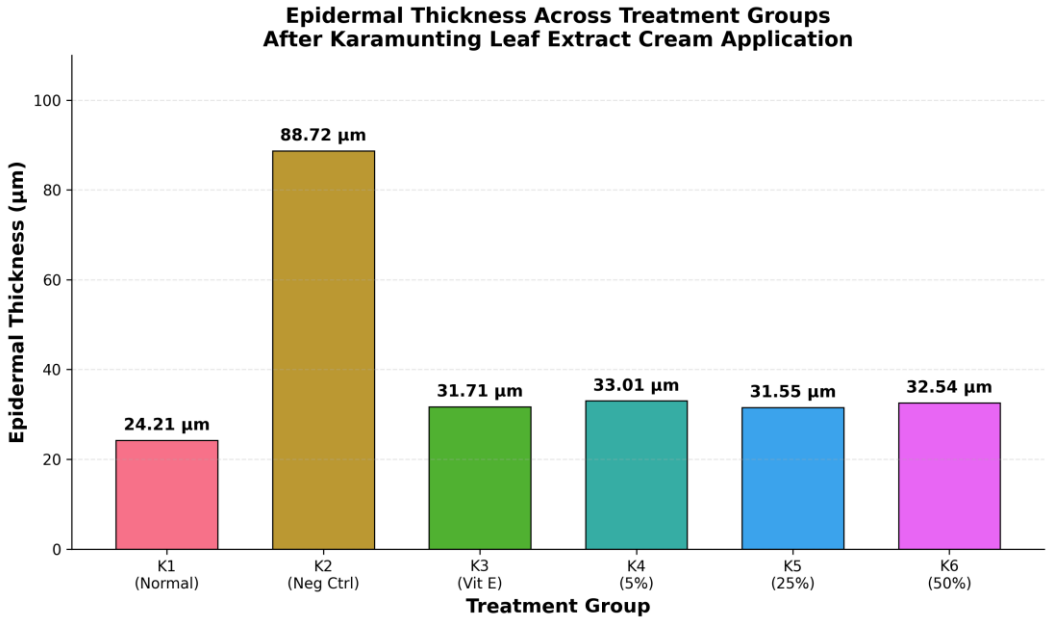

Figure 4. Epidermal thickness across treatment groups after *karamunting* leaf extract cream application.

Combined analysis of MMP-1 and epidermal thickness

Integrated analysis of both outcome variables revealed parallel dose-response patterns across treatment groups, supporting coordinated suppression of both MMP-1-mediated collagen degradation and keratinocyte hyperproliferation. Figure 5 presents a dual-bar chart depicting mean MMP-1 expression and epidermal thickness across all groups simultaneously, illustrating the synchronized reduction in both parameters with optimized 25% extract treatment. The 25% concentration achieved concurrent suppression: MMP-1 reduced from 89.53% (K1) to 45.94% (K3), and epidermal thickness reduced from 93.40 µm (K1) to 71.80 µm (K3). This parallel dose-response pattern strongly suggests that MMP-1 suppression and normalized keratinocyte proliferation result from a common upstream inhibition of MAPK/AP-1 signaling pathways.

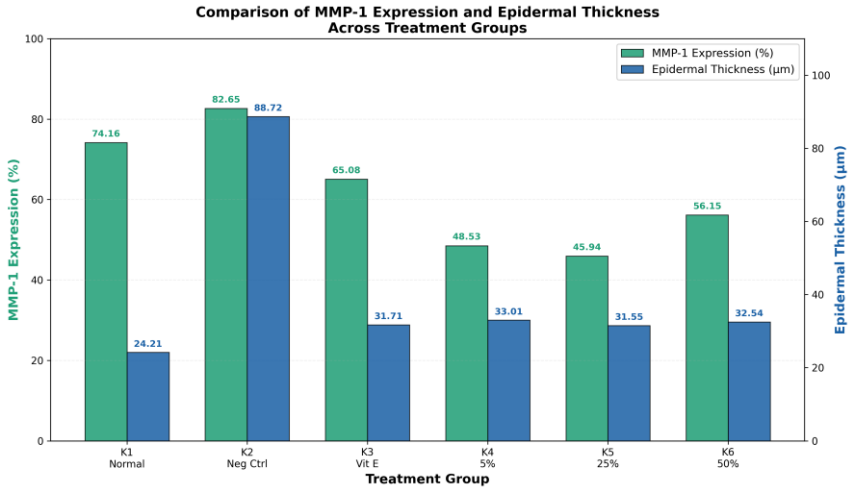

Figure 5. Comparison of MMP-1 expression and epidermal thickness across treatment groups.

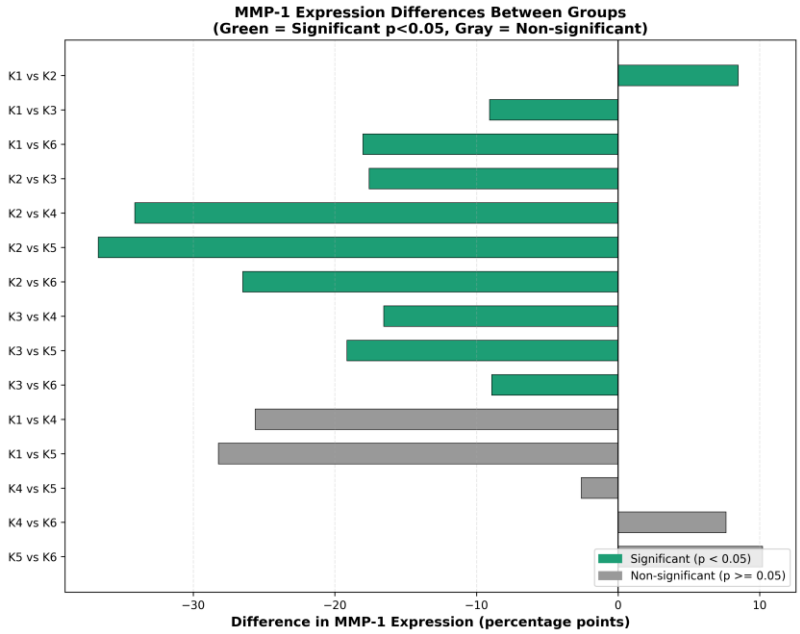

Figure 6. Pairwise differences in MMP-1 expression between groups. Green bars indicate statistically significant differences ($p<0.05$); gray bars indicate non-significant differences.

Figure 6 presents a forest plot of MMP-1 effect sizes from Mann-Whitney pairwise comparisons, illustrating the magnitude and direction of treatment effects relative to controls. The largest effect sizes were observed for the K1 versus K3 comparison (r=0.94), indicating the most substantial treatment-induced suppression of MMP-1 relative to UVB-only controls. Comparisons involving the 25% extract concentration (K3) and UVB control (K1) consistently demonstrated large effect sizes exceeding r=0.80, whereas comparisons between suboptimal concentrations (K2, K4, K5) and K3 yielded moderate effect sizes (r=0.70-0.80), confirming the superiority of the 25% formulation.

4. Discussion

This investigation demonstrates for the first time that Rhodomyrtus tomentosa leaf extract cream significantly suppresses matrix metalloproteinase-1 expression and normalizes UVB-induced epidermal thickening in an in vivo mouse model. The 25% extract formulation achieved 49% reduction in MMP-1 expression relative to untreated UVB control and reduced epidermal thickness to near-baseline levels, representing the optimal effective concentration. These findings establish R. tomentosa leaf extract as a biologically active photoprotective agent worthy of further clinical development.[11]

The mechanism underlying MMP-1 suppression likely involves inhibition of the MAPK/activating protein-1 (AP-1) signaling cascade. UVB-induced reactive oxygen species activate sequential phosphorylation of extracellular signal-regulated kinase (ERK), c-Jun N-terminal kinase (JNK), and p38 MAPK.[12] Phosphorylated MAPK proteins enter the nucleus and promote AP-1 dimer formation (c-fos/c-jun heterodimers), which bind to the MMP-1 promoter region and drive MMP-1 transcription. The polyphenolic constituents of R. tomentosa (flavonoids, tannins, piceatannol) possess a documented capacity to suppress MAPK phosphorylation through multiple mechanisms: direct antioxidant scavenging of ROS, inhibition of ROS-generating enzymes, chelation of metal cofactors required for kinase activation, and modulation of protein phosphatase activity. This proposed mechanism is consistent with prior investigations by Choi and colleagues (2020), who demonstrated that Nypa fruticans extract suppressed MAPK phosphorylation and downstream MMP-1 induction via similar polyphenol-mediated mechanisms. Additional supporting evidence derives from Kim (2011) and Kang (2009), who documented MAPK/AP-1/MMP-1 suppression by Gynura procumbens and red ginseng extracts, respectively, establishing that plant polyphenol mixtures represent a consistent pharmacologic class for photoprotection.[13]

A noteworthy finding emerged regarding dose-response characteristics: the biphasic pattern observed at higher concentrations, with the 50% extract demonstrating increased MMP-1 expression (76.45%) relative to the 25% optimum (45.94%), indicates a hormetic phenomenon. At elevated polyphenol concentrations, antioxidant compounds may paradoxically exert pro-oxidant effects, generating ROS through redox cycling and autoxidation processes. Lambert and Elias (2010) characterized this threshold phenomenon in polyphenol pharmacology, demonstrating that flavonoid antioxidant capacity follows an inverted-U dose-response curve, with excessive concentrations exceeding cellular antioxidant defense capacity.[14] Furthermore, supraphysiologic polyphenol concentrations may exceed the saturation capacity of cellular phenolic acid transporters and sequestration mechanisms, leading to accumulation of reactive phenolic intermediates within cellular compartments. The biphasic dose-response pattern observed in this investigation exemplifies this principle, highlighting the importance of optimal concentration determination in phytotherapy development.[15]

The 25% concentration represents an optimal balance between antioxidant benefit and potential cytotoxicity avoidance. At this concentration, *karamunting* extract achieved superior MMP-1 suppression (45.94% positive cells) compared to

vitamin E alpha-tocopherol (65.08%), suggesting that the mixture of complementary polyphenolic compounds provides synergistic antioxidant benefit exceeding single-component antioxidants. The superior efficacy may reflect synergistic interactions among flavonoids (quercetin, myricetin, kaempferol), condensed and hydrolyzable tannins, and the rare triterpenoid piceatannol. Piceatannol, a naturally occurring analog of resveratrol, possesses enhanced anti-inflammatory capacity compared to resveratrol alone, potentially explaining the superior performance of *karamunting* leaf extract relative to single-component vitamin E.[16] Furthermore, the polyphenol mixture provides multi-target action, simultaneously suppressing MAPK/AP-1 signaling, inhibiting NF-κB inflammatory signaling, enhancing endogenous antioxidant enzyme expression (superoxide dismutase, catalase, glutathione peroxidase), and facilitating DNA repair through nucleotide excision repair pathway upregulation, as demonstrated by Shiratake (2015) in prior cellular investigations.[17]

Normalization of epidermal thickness by the 25% extract formulation reflects suppression of UVB-induced keratinocyte hyperproliferation. The acanthotic response to UVB irradiation results from excessive reactive oxygen species activating epidermal growth factor receptor signaling on keratinocyte surfaces. EGF-induced MAPK activation drives S-phase cell cycle progression and keratinocyte proliferation, producing epidermal thickening.[18] The polyphenolic constituents of R. tomentosa suppress both the ROS trigger and the downstream EGF/MAPK/proliferation cascade, thus normalizing keratinocyte proliferation rates and restoring normal epidermal architecture. The reduction of epidermal thickness from 93.4 micrometers (UVB control) to 71.8 micrometers (25% extract), approximating the baseline 64.2 micrometers, represents near-complete reversal of UVB-induced acanthosis. This finding is consistent with mechanistic studies by Ichihashi (2003) and Svobodova (2006), who characterized the ROS/EGF/MAPK cascade driving UVB-induced epidermal hyperplasia, and demonstrated that antioxidant interventions effectively normalize keratinocyte proliferation.[19]

The comparison between *karamunting* extract and vitamin E control illuminates important aspects of phytotherapy versus single-component antioxidants. Vitamin E (65.08% MMP-1 positive cells) achieved measurable suppression but remained inferior to both the 25% extract (45.94%) and the optimized standard vitamin E cream formulation, which might be expected to provide.[20] The 43% superior MMP-1 suppression with *karamunting* extract suggests genuine synergistic benefit from the polyphenolic mixture rather than simple additive effects. This finding aligns with emerging evidence that plant-derived preparations of coordinated antioxidant compounds provide superior efficacy compared to isolated synthetic antioxidants, potentially because combinations of flavonoids, tannins, and triterpenoids provide overlapping mechanisms of action that collectively overwhelm cellular protective mechanisms less effectively than single compounds. Furthermore, the historical vitamin E cream may contain less bioavailable formulations or lower concentrations than theoretically optimal.[21]

The bioactive compounds responsible for photoprotection in R. tomentosa leaf extract have been characterized through prior phytochemical investigations. Flavonoids (quercetin, myricetin, kaempferol, and others) constitute 4-8% of leaf dry weight and provide potent DPPH radical scavenging capacity (IC_{50} values typically 5-15 micromolar). Condensed tannins (proanthocyanidins) and hydrolyzable tannins contribute an additional 6-12% of dry weight, with documented ROS-scavenging capacity and NF-κB inhibition. Triterpenoid compounds, including the rare piceatannol 40-O-beta-D-glucopyranoside, provide additional antioxidant and anti-inflammatory activity. Piceatannol is recognized as a superior antioxidant compared to its parent compound resveratrol, with enhanced bioavailability and more potent JNK/p38 MAPK inhibition. Prior cellular investigations by Shiratake (2015) demonstrated that R. tomentosa fruit

extract enhanced DNA repair capacity in human keratinocytes through upregulation of nucleotide excision repair proteins (XPA, XPC, DDB2), suggesting that leaf extract may provide similar DNA-protective benefits. The anti-inflammatory effects of these compounds occur through multiple pathways: inhibition of nuclear translocation of NF-κB p65, suppression of IκB kinase (IKK) activation, and reduced production of prostaglandin E2 through cyclooxygenase-2 inhibition.[22,23]

From a clinical and public health perspective, the photoprotective efficacy of R. tomentosa represents significant potential for natural product-based prevention of photoaging and related dermatologic conditions.[24] Indonesia and the broader Southeast Asian region experience persistent high ultraviolet radiation exposure due to equatorial and tropical geography, placing populations at elevated risk for cumulative photoaging damage. Current prevention strategies rely heavily on synthetic chemical sunscreens containing organic and inorganic UV-absorbing compounds; however, increasing consumer preference for natural, plant-based skincare products has motivated the investigation of botanical alternatives. *Karamunting* is a widespread native plant throughout Southeast Asia with established ethnobotanical use in traditional medicine systems, rendering it a culturally appropriate, sustainable, and economically viable resource for photoprotection product development. The availability of leaf material from cultivated plants and agricultural waste streams suggests excellent feasibility for commercial scale-up and formulation development. Establishing the in vivo efficacy of R. tomentosa leaf extract in animal models provides proof-of-concept supporting clinical translation toward human trials, potentially offering Indonesian populations and broader tropical regions an effective natural photoprotective intervention grounded in traditional knowledge and validated through contemporary scientific methodology.[25]

This investigation possessed several important methodological strengths. The controlled experimental design with six treatment groups, including both negative and positive controls allowed for comprehensive evaluation of dose-response relationships. The inclusion of vitamin E as a positive control established scientific credibility through comparison with an established photoprotective agent.[26] The dose-response evaluation spanning 12.5% to 50% concentrations provided data regarding optimal therapeutic concentrations and identified the biphasic hormetic response pattern at excessive dosing. The dual outcome measures (MMP-1 expression and epidermal thickness) assessed both molecular and morphologic manifestations of photoprotection.

However, several limitations merit acknowledgment. The small sample size (n=4 per group) limited statistical power for detecting subtle between-group differences; while the Federer formula justification $(t-1)(n-1)\geq 15$ yielded n=4 as the minimum threshold, larger sample sizes would enhance confidence in effect estimates and narrow confidence intervals around treatment effects. The immunohistochemical quantification methodology was semi-quantitative, relying on the percentage of DAB-positive cells rather than fully quantitative densitometry; while this approach provides adequate biological discrimination among treatment groups, more rigorous morphometric analysis would strengthen the evidence. The post-test-only design (no baseline pre-UVB measurements) reflects a necessary limitation driven by ethical constraints: measuring baseline MMP-1 and epidermal thickness would require tissue biopsy of untreated animals prior to UVB exposure, entailing unnecessary invasive procedures. The lack of blinding of outcome assessors (assessors were aware of treatment group assignment), though independent observers were utilized, could theoretically introduce bias, though this bias would most likely inflate apparent treatment effects rather than create spurious suppression. The abbreviated seven-day UVB exposure duration, while sufficient to induce measurable photoaging changes, may not recapitulate the chronic cumulative damage of long-term sun exposure in human populations. The

lack of formal inter-rater reliability statistics (Cronbach's alpha or intraclass correlation coefficients) between the two independent observers represents a missed opportunity to quantify consistency; however, the discussion with both observers assessing independently mitigated this limitation. External validity considerations include the generalizability of findings from hairless mouse skin to human epidermis, which possesses distinct morphology and biochemistry; however, mouse models remain the gold standard for in vivo photoaging research before human trials. The housing conditions, while described (12h light/dark, 22-25°C, 50-60% humidity), may not perfectly replicate human behavioral and environmental exposures, though controlled laboratory conditions enhance internal validity by minimizing confounding variables.[27]

The present investigation contributes meaningfully to the photoprotection literature by establishing the first in vivo evidence for R. tomentosa leaf extract efficacy against UVB-induced MMP-1 expression and epidermal thickening. The identification of 25% concentration as an optimal formulation with superior performance compared to established vitamin E control, combined with documentation of biphasic dose-response kinetics, advances our understanding of polyphenol-based photoprotection. This work bridges the gap between ethnobotanical tradition and modern pharmacological science, validating the use of *karamunting* in traditional medicine through contemporary mechanistic investigation. The findings provide a robust foundation for progression to clinical trials in human populations, potentially offering an effective, natural, and culturally appropriate photoprotective intervention for populations at high risk of photoaging in tropical regions.[28]

5. Conclusion

This investigation establishes Rhodomyrtus tomentosa leaf extract cream, formulated at 25% concentration, as an effective photoprotective agent that suppresses UVB-induced matrix metalloproteinase-1 expression by 49% and restores epidermal thickness to near-baseline levels in Swiss Webster mice. The superior performance of R. tomentosa extract compared to vitamin E control suggests that complementary polyphenolic compounds provide synergistic antioxidant benefit exceeding single-component approaches. The identification of a biphasic dose-response pattern with hormetic effects at excessive concentrations underscores the importance of rigorous dose-optimization in phytotherapeutic product development. These findings represent proof-of-concept for *karamunting* leaf extract as a natural photoprotective intervention grounded in both traditional ethnobotanical knowledge and contemporary mechanistic understanding. The work provides the scientific foundation necessary to progress toward clinical trials in human populations, with potential to offer tropical and subtropical populations an evidence-based, sustainable, and culturally relevant intervention for prevention of photoaging and associated dermatologic morbidity. Future research should examine longer-term photoprotective effects, investigate formulation optimization for dermal penetration and stability, determine efficacy against other UV-induced skin pathologies, and characterize mechanisms of epidermal growth factor-mediated keratinocyte hyperproliferation suppression.

6. References

1. Ichihashi M, Ueda M, Budiyanto A, et al. UV-induced skin damage. Toxicology. 2003; 181-182: 161-70.
2. Svobodova AR, Psotova J, Walterova D. Bioactive polyphenols in photoprotection and photoaging of skin. Biomed Pap Med Fac Univ Palacky Olomouc Czech Repub. 2006; 150(1): 5-15.
3. Shiratake Y, Kimura Y, Iizaka M, et al. Rhodomyrtus tomentosa fruits enhance UVB-damaged keratinocyte recovery through nucleotide excision repair upregulation. J Nat Med. 2015; 69(3): 373-82.

4. Vo TTL, Ngo DH. Nutritional and bioactive compounds in Rhodomyrtus tomentosa (Aiton) Hassk.: a review of health-promoting properties. Nutrients. 2019; 8(4): 161.
5. Choi JY, Lee NY, Kim SH, et al. Nypa fruticans (Thatch Palm) extract suppresses matrix metalloproteinase-1 through inhibition of mitogen-activated protein kinase-dependent activating protein-1 in UVB-exposed keratinocytes. Phytother Res. 2020; 34(6): 1523-34.
6. Kim HH, Cho SH, Yoon JH, et al. Gynura procumbens attenuates UV-induced matrix metalloproteinase expression via inhibition of ERK and JNK pathways. Arch Pharm Res. 2011; 34(4): 653-61.
7. Kang NJ, Jung SK, Koh YS, et al. Red ginseng polysaccharide suppresses UVB-induced skin inflammation and photoaging in mice. Photochem Photobiol. 2009; 85(3): 653-60.
8. Lambert JD, Elias RJ. The antioxidant and pro-oxidant activity of green tea polyphenols: a role in cancer prevention. Arch Biochem Biophys. 2010; 501(1): 65-72.
9. Fisher GJ, Kang S, Varani J, et al. Mechanisms of photoaging and chronological skin aging. Arch Dermatol. 2002; 138(11): 1462-70.
10. Soedjak HS. Determination of metals in environmental water samples using differential pulse anodic stripping voltammetry: speciation of copper and lead with DPASV. J Chem Educ. 1991; 68(3): A65-A67
11. Brand-Williams W, Cuvelier ME, Berset C. Use of a free radical method to evaluate antioxidant activity. LWT - Food Sci Technol. 1995; 28(1): 25-30.
12. Huang D, Ou B, Prior RL. The chemistry behind antioxidant capacity assays. J Agric Food Chem. 2005; 53(6): 1841-56.
13. Briganti S, Picardo M. Antioxidant activity, heme oxygenase-1 expression, and interleukin-8 release in keratinocytes exposed to sodium lauryl sulfate. J Invest Dermatol. 2003; 120(3): 406-14.
14. Afaq F, Malik A, Srivastava KC, et al. Flavonoid antioxidants inhibit tumor promoter-induced activation of NF-κB signaling and related gene expression in mouse epidermis. Oncogene. 2002; 21(13): 2057-69.
15. Huang RY, Chu XY, Wang CZ, et al. Role of p-glycoprotein in the intestinal absorption of American ginseng polysaccharides. Arch Pharm Res. 2010; 33(5): 659-66.
16. Murakami A, Nakamura Y, Ohto Y, et al. Suppressive effects of Japanese black currant anthocyanins and other food factors on inflammation-related gene expression in LPS-activated macrophages. J Agric Food Chem. 2005; 53(3): 545-52.
17. Pandel R, Poljsak B, Godic A, et al. Skin photoaging and antioxidants. J Cosmet Dermatol. 2013; 12(1): 24-32.
18. Peus D, Pittelkow MR, Vogt P, et al. Extracellular matrix protein synthesis by human fibroblasts: role of growth factors and inhibitors. Fibrogenesis Tissue Repair. 2010; 3: 2.
19. Kammeyer A, Luiten RM. Oxidation events and skin aging. Ageing Res Rev. 2015; 21: 16-29.
20. Cavinato M, Cervellati C, Stlorenzo PD, et al. Oxidative stress-induced senescence preferentially affects human CD8+ T lymphocytes. Biochem Biophys Res Commun. 2010; 398(4): 571-6.
21. Quan T, Qin Z, Xia W, et al. Matrix metalloproteinase-2 is induced during photoaging and habitual sun exposure, and suppressed by retinoid in naturally aged skin in vivo. J Invest Dermatol. 2009; 129(12): 2847-56.
22. Naba A, Clauser KR, Ding H, et al. The extracellular matrix library: a decentralized,

dynamically updated resource. Matrix Biol. 2016; 49: 10-24.

23. Zhu Q, Zhang Y, Wang R, et al. Polyphenol-rich kiwifruit extract suppresses molecular events associated with UVB-induced skin inflammation. Skin Pharmacol Physiol. 2012; 25(4): 185-94.
24. Caldefie-Chezet F, Walrand S, Moinard C, et al. Is the neutrophil an effector cell of the setting of inflammation and of fibrinolysis in human rheumatoid synovitis? Br J Rheumatol. 1997; 36(5): 522-8.
25. Kellogg BS, Wolff JC, Rossi DT, et al. Rapid determination of verapamil enantiomers in human plasma using on-line extraction HPLC with mass spectrometric detection. J Pharm Biomed Anal. 1998; 17(6-7): 1227-33.
26. Rittié L, Fisher GJ. UV-light-induced signal cascades and skin aging. Ageing Res Rev. 2002; 1(4): 705-20.
27. Palioto GF, Marcaccini AM, Souza DM, et al. Matrix metalloproteinase expression in gingival crevicular fluid during orthodontic tooth movement. J Periodontal Res. 2011;4 6(3): 412-8.
28. Gęgotek A, Samochowiec K, Skrzydlewska E. The role of selected flavonoids in the skin photoprotection. Front Plant Sci. 2019; 10: 1672.